



48th CIRP Conference on MANUFACTURING SYSTEMS - CIRP CMS 2015

Laser marking of titanium coating for aerospace applications

C. Velotti^a, A. Astarita^{a,*}, C. Leone^{a,b}, S. Genna^b, F. Memola Capece Minutolo^a, A. Squillace^a^aDepartment of Chemical, Materials and Production Engineering, University of Naples Federico II, P.le Tecchio 80, 80125 Naples, Italy^bCIRTIBS Research Centre, University of Naples Federico II, P.le Tecchio 80, 80125 Naples, Italy* Corresponding author. Tel.: +39 081 768 2555; fax +39 . 0817682362 E-mail address: antonello.astarita@unina.it

Abstract

In the aerospace industry, in order to ensure the identification and the traceability of the products, high repeatability, non-invasive and durable marking processes are required. Laser marking is one of the most advanced marking technologies. Compared to traditional marking processes, like punches, microdot, scribing or electric discharge pencil etcher, laser marking offers several advantages, such as: non-contact working, high repeatability, high scanning speed, mark width comparable to the laser spot dimension, high flexibility and high automation of the process itself. In order to assure the mark visibility for the component lifetime, an appropriate depth of the mark is required. In this way, a stable behaviour is ensured also when the component operates in aggressive environments (i.e. in presence of oxidation, corrosion and wear phenomena). The mark depth is strongly affected by the laser source kind and by the process parameters, such as average power, pulse frequency and scanning speed. Moreover, an excessive mark penetration could cause stress concentrations and reduce the fatigue life of the component. Consequently, an appropriate selection of the process parameters is required in order to assure visibility and to avoid excessive damage. Cold Spray Deposition (CSD) is a relative new technology that allows to produce surface coatings without significant substrate temperature increasing. In aeronautics fields this technology is useful to coat materials sensible to temperature, such as solution tempered aluminum alloy, with a titanium layer. Aim of the work is to characterize the laser marking process on CSD Ti coating, in order to study the influence of the laser marking process parameters (pulse power and scanning speed), on the groove geometry of the marking. The experimental marking tests were carried out through a 30 W MOPA Q-Switched Yb:YAG fibre laser; under different process conditions. The groove geometry was measured through a HIROX HK9700 optical microscope. The results showed the effectiveness of the laser process to produce high quality marks on the titanium layer. Moreover, a correlation between the process parameters and the mark's geometry was clearly observed.

© 2015 The Authors. Published by Elsevier B.V. This is an open access article under the CC BY-NC-ND license

[\(http://creativecommons.org/licenses/by-nc-nd/4.0/\)](http://creativecommons.org/licenses/by-nc-nd/4.0/).

Peer-review under responsibility of the scientific committee of 48th CIRP Conference on MANUFACTURING SYSTEMS - CIRP CMS 2015

Keywords: Cold Spray, Coating, Titanium, Laser Marking.

1. Introduction

The modern industry, in order to preserve, protect, promote and enhance the value of their activities, uses various methods of obtaining traceability characteristics, for preventing and reducing the forgery attempts, but also for the improvement of the quality and safety of its products. Direct laser marking is a widely used flexible and modern method to obtain permanent marks containing traceability and identification information: alphanumeric strings of characters, logos, barcodes and Data Matrix codes [1]. In particular, in aerospace industry, in order to ensure the identification and the traceability of the

products, high repeatability, non-invasive and durable marking processes are required [2-3]. Compared to the traditional marking processes, like punches, microdot, scribing or electric discharge pencil etcher, laser marking offers several advantages, such as: non-contact working, high repeatability, high scanning speed, a mark width comparable to the laser spot dimension, high flexibility and high automation of the process itself [4]. In order to assure the mark visibility for the component lifetime, an appropriate depth of the mark is required [5-6]. In this way, a stable behaviour is ensured also when the component operates in aggressive environments (i.e. in presence of oxidation,

corrosion and wear phenomena). The mark depth is strongly affected by the laser source and by the process parameters, such as mean power, pulse frequency and scanning speed [6]. Moreover, an excessive mark penetration could be cause of stress concentrations and reduce the fatigue life of the component [6-7]. Consequently, an appropriate selection of the process parameters is required in order to assure visibility and to avoid excessive damage.

In the last decade titanium and its alloys are finding a widespread increasing use in the aerospace industry due to their lightweight, coupled with high corrosion resistance and good compatibility with carbon fiber reinforced plastics [8]. On the other hand, the use of titanium alloys is limited by the high costs of the raw material, the difficulty of machining and the general complexity of manufacturing processes. The application of Ti coatings on other bulk metals, such as the high strength aluminium alloys used in aeronautics, could be an intriguing solution to produce light, cheap components with the high superficial properties typical of titanium alloys.

An effective technique that could be used to produce titanium coating on aluminium components is the Cold Gas Dynamic Spray (CGDS), that is an additive technology [9] that makes use of a converging/diverging nozzle (known as De Laval nozzle) and a high pressure, heated gas source (usually nitrogen) to create a supersonic gas flow. Metallic particles, usually in the size range of 10–100 μm , are injected into this gas flow and propelled to supersonic velocities. Typical particle velocities range from 500 to 1000 m/s and a high kinetic energy causes the impingement of the particles onto the substrate [10]. Depending on the material and particle speed, the particles will either rebound from the substrate (with or without erosion) or bond with the substrate [11]. The speed at which bonding is achieved (it is referred to as critical velocity and depends on the particles size), depends on the particles distribution and on the substrate material. Macroscopic plastic deformation, resulting from the high impact velocity, is generally believed to be the main bonding mechanism for metallic coatings deposited on metallic substrates [12–13]. The high impact momentum of the particles causes mechanical interlocking varying, depending on the application conditions and the metals employed. In this process, coating deposition occurs at relatively low temperatures, compared to other spray technologies. Moreover, during the process, the sprayed particles remain in solid state. The coatings produced through this technology, exhibit remarkably high densities and conductivities, good corrosion resistance and a high hardness due to their cold worked microstructure [14]. The process provides a solution for applications where conventional metal spraying processes, such as flame, arc, plasma and HVOF spraying, are inappropriate, in which problems such as coating porosity, oxidation and low adhesion may occur [15-16]. Furthermore, this process could be the only chance to produce coatings of solution tempered aluminium alloys, due to the presence of an aging temperature that is easily reached during the thermal spray processes.

The coupling of the aluminium lightweight and economy with the high corrosion resistance of titanium will be useful in the production of new generation aircrafts. On these premises

the laser marking process, in order to ensure the traceability of components, has to be studied. To authors best knowledge, there are no papers in literature dealing with this topic. The aim of the present paper is the study of the laser marking, through a 30 W MOPA Q-Switched Yb:YAG fibre laser, of titanium cold sprayed coatings. In particular it was studied: i) the effective processing area; ii) the influence of the process parameters on the marking features.

2. 2. Material, equipment and experimental procedures

2.1. Materials and coating production procedures

Commercially pure (grade 2) titanium particles with a mean granulometry of 40 μm were deposited onto an AA 2024-T3 plates 2 mm thick. The chemical composition and the main properties of both grade 2 titanium and AA 2024-T3 are fully available in literature and are not here reported for the sake of brevity. Marking tests were also carried out on grade 2 Titanium rolled sheets 1 mm thick.

Commercial cold spray facility DYMET403J (Obninsk-Center for Powder Spraying) was used for spraying. In order to avoid titanium particles oxidation during the spraying process, the deposition was carried out adopting Helium as carrier gas [17-18]. A round-shaped exit nozzle, 4.8 mm in final diameter, was adopted. In Fig. 1, a sketch of low pressure gas dynamic spray process is reported.

The parameters for the spraying process were chosen taking into account the previous literature [19]. In particular the particles were sprayed at a velocity of 680 m/s with Helium gas at 600 °C while the chamber pressure was about 15 bars. Under these conditions, a superficial layer of cold sprayed titanium powder, 5 mm thick, was obtained on the substrate of aluminium plates. After the deposition the titanium coating was milled in order to obtain a regular surface and a thickness of 0.3 mm.

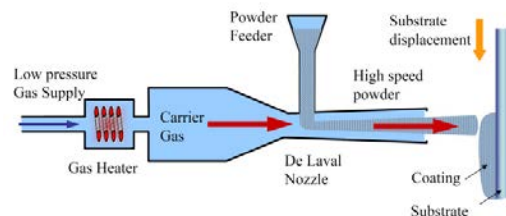


Fig. 1. Low pressure gas dynamic spray process schematization.

2.2. Laser marking process

The experimental tests were performed using a 30 W MOPA Q-Switched Yb:YAG fibre laser. The laser beam was moved by means of a galvanometric mirrors system and focused by a "flat field lens" on the plate surface. The laser system was computer controlled, allowing the generation of the geometric patterns and the set up of the process parameters: average power (Pa), pulse frequency (F), scan speed (Ss). Table 1 shows the detailed characteristics of the laser system.

In the present work this kind of laser was chosen because of the good absorption of metals under investigation at the Yb:YAG wavelength ($\lambda=1064$ nm), the high pulse power, Pp, (up to 20 kW), the possibility to have the nominal power

(30W) at all the frequencies and for the high efficiency and lower power consumption (120W) compared to the traditional Nd:YAG or CO₂ laser source. The latter characteristic is very important when environmental as well as process sustainability are considered. In the adopted laser, for a fixed average power, pulse energy (Pe) and pulse power (Pp) depend on pulse frequency, as reported in Fig. 2. Pulse energy was calculated as the ratio between average power and pulse frequency, and pulse power as the ratio between pulse energy and duration. The average power was measured using a power meter (F150A-SH thermal head and a NOVA display by OPHIR). Pulse energy and pulse power play a central role in laser machining and micromachining since they determine the fluence (energy density) and the irradiance (power density), and then the laser beam-material interaction mode and the amount of machined volume [20-25]. On the other hand, it is worth noting that pulse energy and pulse power differ only by a constant (the pulse duration), while the frequency and the scan speed affect the so-called overlapping factor (R%) that is another critical parameter in pulse laser applications.

In this work the attention was focussed on two process parameters: the scan speed and the maximum pulse power (Pp). A wide range of these process parameters was investigated in order to obtain: i) the effective processing window; ii) an evaluation of the influence of the process parameters on the mark geometry. In particular the following values of the process parameters under investigation were adopted: Scan speed [mm/s]: 25; 50; 100; 200; 400; 600; 800; 1000; 1500; 2000. Pulse power [kW]: 10; 15; 20.

For each set of the process parameters three different markings were carried out. The others process parameters were kept constant in all the tests. The whole experimental campaign was repeated even on a grade 2 titanium plate, this in order to better understand and study the phenomena occurring during the marking of cold sprayed layers.

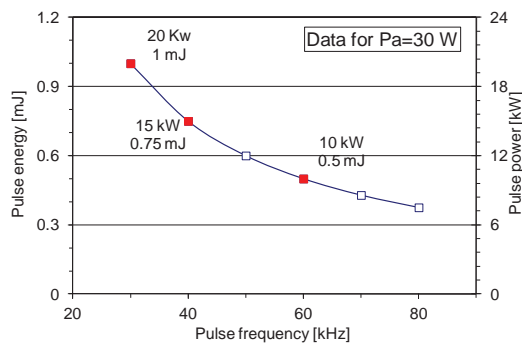


Fig. 2. Pulse energy (Pe) and pulse power (Pp) as a function of pulse frequency for an average power of 30W. The adopted experimental conditions are highlighted by the close dots.

2.3. Experimental measurements

After the laser processing, in order to measure the mark geometry and the heat affected zone extension, the samples were cut, embedded in epoxy resin and mechanically polished by mean of a polishing machine and, finally, etched with the Kroll's reagent. The sections were, then, observed through a HIROX KH8700 microscope to measure the geometrical features of the markings. In particular, the maximum

penetration depth (Dp) and the maximum width (W) of the marks were used to evaluate the mark geometry. In figure 3, two images of how Dp and W were measured are reported. It is worth to notice that, as long as information on the overall damage caused by the mark is required, the use of Dp is preferable to the measure of the mark depth as often proposed in bibliography [2-6]. In figures 4 and 5 images of the mark are reported for the titanium cold sprayed layer and titanium sheet respectively.

Table 1. Laser system characteristics.

Characteristics	Symbol	Value	Unit
Wavelength	λ	1064	[nm]
Nominal average power	Pa	30	[W]
Maximum pulse energy*	Pe	1	[mJ]
Maximum peak power*	Pp	20	[kW]
Pulse frequency	F	30÷80	[kHz]
Pulse duration	Dr	50	[ns]
Scan speed	Ss	1 ÷ 5000	[mm/s]
Mode	TEM	00	--
	M ²	1.2 ÷ 1.5	--
Focused spot diameter **	--	≈ 80	[μm]
Beam motion	by galvo mirror scanner		--
Working area**		100 x 100	[mm ²]
Power consumption***		120	[W]

*At Pa = 30 W and F = 30 kHz.

** For a "Flat field" lens, with a focal length of 160 mm.

*** At the max. power output.

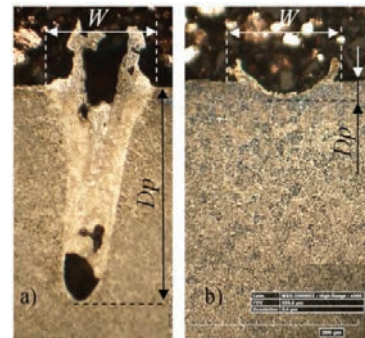


Fig. 3. Entities measured to study the quality of the markings: mark width (W), maximum penetration depth (Dp) on titanium sheet obtained at Pp=20 kW and (a) Ss=25 mm/s; (b) Ss=200 mm/s,



Fig. 4. Macrograph of the markings on the titanium cold sprayed layer performed at Pp=20 kW.



Fig. 5. Macrograph of the markings on the titanium sheet performed at $P_p=20$ kW.

3. Results and discussion

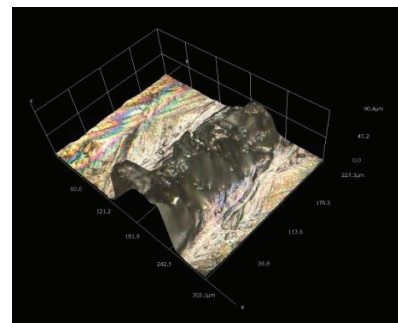
3.1. Processing map

The grooves produced by marking exhibit the configurations shown in Figure 6. From the figure three different states can be identified:

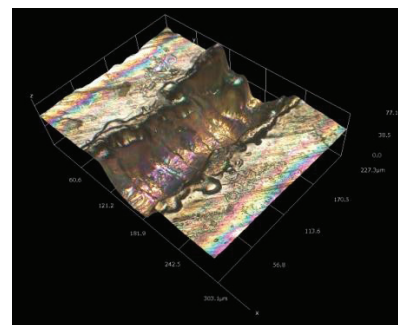
- Irregular groove due to a too high energy released for unit length. The absorbed energy melts the material and heats it up to the vaporisation temperature. The vaporised material forms hot plasma. The pressure reached in the plasma plume is able to pull out part of the molten material far away from the machined area. Due to the too high released energy, high penetration is obtained. However, under this condition, the plasma is not able to eject all the molten material, so the latter is accumulated on the groove edge.
- Regular and effective mark. The energy released for unit length is able to generate a well visible track. The released energy is not enough to generate excessive penetration, so the recoil pressure is able to eject all the molten material out of the kerf. However, a thin layer of resolidified materials remains smeared on the groove surface.
- Regular but inadequate groove. The energy released is too weak to produce an effective penetration into the material. The mark is visible, but it is too shallow to give a permanent and durable marking.

Since the process purpose is to obtain a low invasive and durable mark, it can be stated that the best process conditions are those corresponding to the (b) state. In order to detect the process conditions that allow obtaining marking corresponding to the (b) state, the different states were reported against the scan speed and the pulse power in Figs. 7-8 for the titanium sheet and the coating, respectively. From the figures, the state, regardless of the adopted peak power, depends only by the scanning speed and the materials type: for scan speed lower than 200 mm/s the high heat input leads to (a) state. Conversely, for scan speed higher than 800 mm/s and 1000 mm/s for the titanium sheet and titanium coating, respectively, the heat input was too low to produce an effective mark; resulting in (c) state. So, the effective processing area is included in the scan speed range between 200 and 800 mm/min for both the materials. Moreover, comparing Fig. 7 to Fig. 8 and considering only the states, it is possible to affirm that the processing area is about the same for both the materials. The 3D reconstruction of the mark and the classification according to the three states are useful to detect how the process parameters affect the mark appearance. However, since the aim of the work is to study the influence of the process parameters on the marking features and the damages produced into the materials, the maximum depth

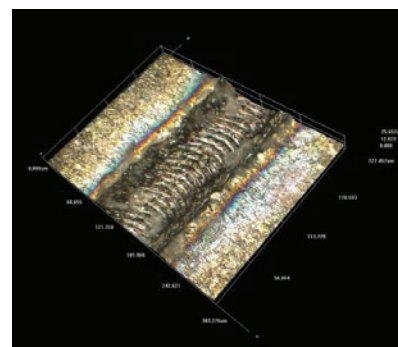
(penetration depth) and width of the mark have to be considered.



(a)



(b)



(c)

Fig. 6. Typical appearance of the mark. 3D reconstruction of marks obtained at: a) $P_p=20$ kW; $S_s=25$ mm/s; b) $P_p=10$ kW; $S_s=600$ mm/s; c) $P_p=10$ kW; $S_s=2000$ mm/s.

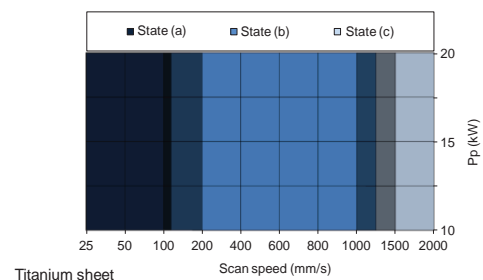


Fig. 7. Processing window for the titanium sheet.

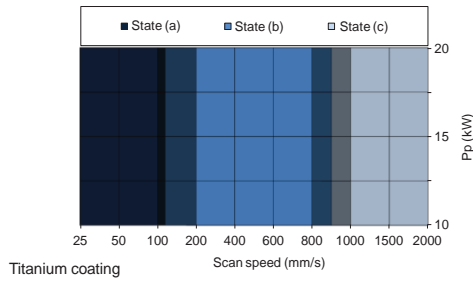


Fig. 8. Processing window for the titanium coating.

Then, in order to obtain quantitative information, investigations were carried out on the marks penetration depth and width, according to that reported in Fig. 3.

3.2. Groove geometry and HAZ extension

In figures 9-10 the total penetration depth are reported against the scanning speed at different pulse power for the titanium sheet and coating, respectively. In the diagrams the dashed red line represents the limit $Dp=5 \mu\text{m}$. Below this value, the discrimination of the mark depth is very hard to perform. From the figures, as expected, the maximum depth decreases as the speed increases. The decrease is very fast in the range $Ss=25\text{--}200 \text{ mm/s}$. For Ss higher than 200 mm/s , the decrease proceeds more slowly. This is consistent with that observed in [6]. Regarding the effect of the pulse power the increase of the Pp produces, for both materials, a decrease of the maximum penetration depth. Moreover, the coating shows a data scattering that is always higher with respect to the one shown by the sheet. The effect of the Pp is unexpected. A possible explanation is that the increase of the Pp is obtained by decreasing the pulse frequency. Then, lower Pp corresponds to high pulse frequency or high overlapping factors. Under these conditions, the reduction of the time between two consecutive pulses (pulse-off cooling), does not permit an effective cooling of the area around the mark. Consequently, the heat is accumulated in the region and, thus, produces an increase of the mark penetration.

In figures 11-12, the overall marking width is reported against the scanning speed at different pulse power for the titanium sheet and coating, respectively. From the figures, increasing Ss , the total width of the marking tends to decrease rapidly, until it reaches a value of about $100 \mu\text{m}$ (obtained at a Ss of 200 and 400 mm/s for the sheet and the coating, respectively). Beyond these values, the width continues to decrease increasing the speed, but with a much slower progression. Also in this case, it is possible to observe a greater dispersion of the data in the case of the coating, compared to the sheet. It is possible that the data scattering observable for the coating is due to the discontinuous nature of the coating, this is reflected in the thermal properties of the material. As a consequence, the coating shows a more discontinuous behaviour. In order to compare the coating to the massive material, the penetration depth and the width were reported as a function of the scan speed, irrespective of the Pp , for both materials in Figs 13 and 14 respectively.

From the Fig. 13 it is possible to note that the coating shows a highest penetration depth if compared to the bulk material. While, comparing the mark width, excluding the data scattering, it is not possible to distinguish between the two materials.

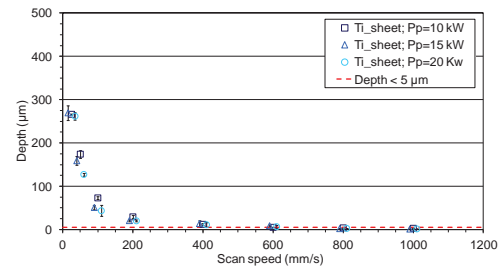


Fig. 9. Mark depths against scanning speed for the different pulse power. Titanium sheet.

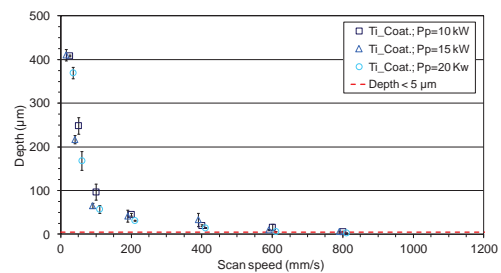


Fig. 10. Mark depths against scanning speed for the different pulse power. Titanium coating.

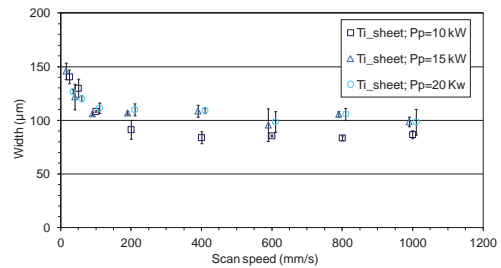


Fig. 11. Mark widths against scanning speed for the different pulse power. Titanium sheet.

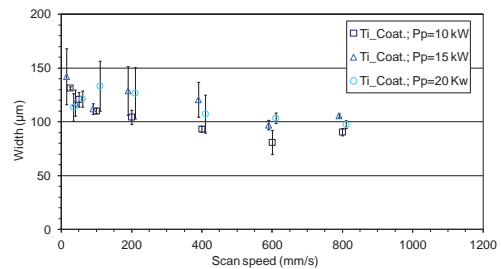


Fig. 12. Mark widths against scanning speed for the different pulse power. Titanium coating.

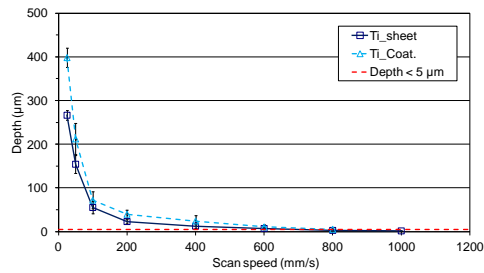


Fig. 13. Mark depth against scanning speed: comparison between the titanium sheet and titanium coating.

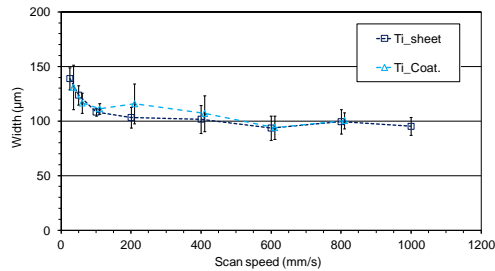


Fig. 14. Mark width against scanning speed: comparison between the titanium sheet and titanium coating.

4. Conclusions

On the basis of the experimental campaign carried out and above described, the following considerations could be drawn:

- The feasibility of the process is mainly ruled by the heat input, in particular three different states were observed: (a) irregular mark due to a too high heat input; (b) regular and effective mark; (c) regular but inadequate mark due to a low heat input.
- Considering only the mark state (b), it is possible to affirm that the processing window was about the same for both the titanium sheet and the cold sprayed coating.
- However, the coating shows a penetration depth that is highest compared to the one obtained on the massive materials.
- The results have also highlighted the importance of the penetration depth as index for the evaluation of the mark geometry.

References

- [1]. Jangsombatsiri W., Porter J.D., Laser Direct-Part Marking of data matrix symbols on carbon steelsubstrates - Journal of Manufacturing Science and Engineering, 2007; 129/3: 583-591.
- [2]. Qiu H., Bao W., Lu C., Investigation of laser parameters influence of direct-part marking data matrix symbols on aluminum alloy, Applied Mechanics and Materials, 2012; 141/1: 328-333.
- [3]. Li C.L., OFAT experimental study of laser direct-part marking of data matrix symbols on titanium alloys, Advanced Materials Research, 2014; 915-916: 1027-1031.
- [4]. Ready J.F. et al., LIA Handbook of laser materials processing. New York, Springer Verlag, 2001.
- [5]. Qi J., Wang K.L., Zhu Y.M., A study on the laser marking process of stainless steel. J. Material Processing Technology, 2003; 139/1-3: 273-276.
- [6]. Leone C., Genna S., Caprino G., De Iorio I., AISI 304 stainless steel marking by a Q-switched diode pumped Nd:YAG laser, J. of Materials Processing Technology, 2010; 210/10: 1297-1303.
- [7]. Nardi A.T., Smith S.L., Laser generated crack-like features developed for assessment of fatigue threshold behavior, ASTM Special Technical Publication, 2009; 1508 STP: 592-605.
- [8]. Welsch G., Boyer R., Collings E.W., Material properties handbook: Titanium Alloys. ASM International, 1993, 713-715.
- [9]. Irissou E., Legoux J. G., Ryabinin A. N., Jodoin B., and Moreau C., Review on Cold Spray Process and Technology: Part I-Intellectual Property, J. of Thermal Spray Technology, 2008; 17/4: 495-516.
- [10]. Schmidt T., Gaertner F., Kreye H., New Developments in Cold Spray Based on Higher Gas and Particle Temperatures, J. of Thermal Spray Technology, 2006; 15/ 4: 488-494.
- [11]. Astarita A., Durante M., Langella A., Montuori M., Squillace A., Mechanical characterization of low pressure cold-sprayed metal coatings on aluminium, Surface and Interface Analysis, 2013; 45/10: 1530-1535.
- [12]. Morgan R., Fox P., Pattison J., Sutcliffe C., O'Neill W., Analysis of cold gas dynamically sprayed aluminium deposits, Materials Letters; 2004; 58/7-8: 1317-1320.
- [13]. Marrocco T., McCartney D., Shipway P., Sturgeon A., Production of titanium deposits by cold-gas dynamic spray: Numerical modeling and experimental characterization, J. of Thermal Spray Technology, 2006; 15/2: 263-272.
- [14]. Irissou E., Legoux J. G., Arsenault B., Moreau C., Investigation of Al-Al₂O₃ Cold Spray Coating Formation and Properties, J. of Thermal Spray Technology, 2007; 16/5-6: 661-668.
- [15]. Astarita A., Durante M., Langella A., Squillace A., Elevation of tribological properties of alloy Ti - 6% Al - 4%V upon formation of a rutile layer on the surface, Metal Science and Heat Treatment; 2013; 54/11: 662-666.
- [16]. Astarita A., Durante M., Langella A., Squillace A., Improving of steel superficial properties through thermal sprayed coatings, Int. J. Surface Science and Engineering, 2013; 7/4: 366-381.
- [17]. Astarita A., Genna S., Leone C., Memola Capece Minutolo F., Paradiso V., Squillace A., Ti-6Al-4V Cutting by 100W fibre laser in both CW and modulated regime, Key Engineering Materials, 2013; 554-557: 1835-1844.
- [18]. Astarita A., Genna S., Leone C., Memola Capece Minutolo F., Paradiso V., Squillace A., Laser Cutting of Aluminum Sheets with a Superficial Cold Spray Titanium Coating, Key Engineering Materials, 2014; 611-612: 794-803.
- [19]. Moy C.K.S., Cairney J., Ranzi G., Jahedi M., Ringer S.P., Investigating the microstructure and composition of cold gas-dynamic spray (CGDS) Ti powder deposited on Al 6063 substrate, Surface & Coatings Technology, 2010; 204: 3739-3749.
- [20]. Lutey A. H. A., Fortunato A., Ascari A., Carmignato S., Leone C., Laser Cutting of Lithium Iron Phosphate Battery Electrodes: Characterization of Process Efficiency and Quality, Optics & Laser Technology, 2015; 65: 164-174.
- [21]. Astarita A., Genna S., Leone C., Memola Capece Minutolo F., Paradiso V., Squillace A., Ti-6Al-4V Cutting by 100W fibre laser in both CW and modulated regime, Key Engineering Materials, 2013; 554-557: 1835-1844.
- [22]. Leone C., Genna S., Tagliaferri V., Fibre laser cutting of CFRP thin sheets by multi-passes scan technique, Optics and Lasers in Engineering, 2013; 53: 43-50.
- [23]. Leone C., Papa I., Tagliaferri F., Lopresto V., Investigation of CFRP laser milling using a 30W Q-switched Yb:YAG fiber laser: Effect of process parameters on removal mechanisms and HAZ formation, Composites Part A: Applied Science and Manufacturing, 2014; 55: 129-142.
- [24]. Leone C., Quadri F., Santo L., Tagliaferri V., Trovalusci F., Nd:YAG laser sculpture of WC punches for micro-sheet forming, Key Engineering Materials, 2007; 344: 783-789.
- [25]. Genna S., Leone C., Lopresto V., Tagliaferri V., Experimental investigation on laser milling of PMMA sheet, AIP Conference Proceedings, 2014; 1599: 242-245.